33rd Annual International Conference of the IEEE EMBS
Boston, Massachusetts USA, August 30 - September 3, 2011

Automated Detection of Red Lesions from Digital Colour Fundus Photographs

Hussain F. Jaafar, Asoke K. Nandi and Waleed Al-Nuaimy

Abstract— **Earliest signs of diabetic retinopathy, the major cause of vision loss, are damage to the blood vessels and the formation of lesions in the retina. Early detection of diabetic retinopathy is essential for the prevention of blindness. In this paper we present a computer-aided system to automatically identify red lesions from retinal fundus photographs. After pre-processing, a morphological technique was used to segment red lesion candidates from the background and other retinal structures. Then a rule-based classifier was used to discriminate actual red lesions from artifacts. A novel method for blood vessel detection is also proposed to refine the detection of red lesions. For a standarised test set of 219 images, the proposed method can detect red lesions with a sensitivity of 89.7% and a specificity of 98.6% (at lesion level). The performance of the proposed method shows considerable promise for detection of red lesions as well as other types of lesions.**

I. Introduction

Diabetes occurs when the level of glucose in the blood is higher than normal. Over several years diabetes can damage the blood vessels of the retina causing what is called diabetic retinopathy (DR) and is the major cause of poor vision [1]. If the disease is detected in the early stages, treatment can slow down the progression. The earliest signs of DR are damage to the tiny blood vessels and the formation of lesions. Signs of DR include bright lesions such as hard exudates and cotton wool spots and red lesions such as microaneurysms and hemorrhages. This paper is concerned only with the red lesions because they are the earliest signs of DR. Red lesions are small swellings that form on the side of the tiny blood vessels. These swellings may break causing blood to leak into nearby tissue [2].

Colour fundus images, such as the one shown in Fig.1, are used to detect DR in a noninvasive manner for large scale screening. More accurate quantification of the progress of DR can be made by identifying red lesions in such retinal images. They represent the specific marker for the existence of co-existent retinal oedema, the major cause of blindness. Some red lesions may appear in association with larger vessels or they may look similar to other retinal pathologies. So, the identification of red lesions is not easy task. Manual detection is time-consuming and often susceptible to observer error. Hence, a computer-aided system would offer fast and consistent diagnosis aid to specialist inspection and assist the clinician to take timely treatment decisions.

Manuscript received April 14, 2011.

Hussain F. Jaafar , Asoke K. Nandi and Waleed Al-Nuaimy are with the Department of Electrical Engineering and Electronics, University of Liverpool, Brownlow Hill, Liverpool, L69 3GJ, UK, (e-mails: h.jaafar, a.nandi, wax @liverpool.ac.uk).

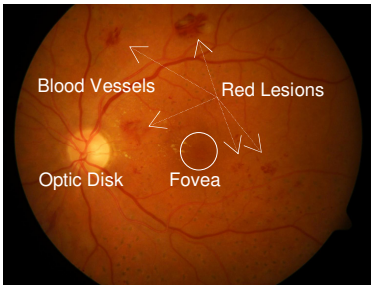

Fig.1 A colour fundus image containing DR

Several researchers have proposed different techniques for red lesion detection, such as Niemeijer *et al.* [3] who proposed a red lesion detection method based on pixel classification to separate vasculature and red lesions from the background and a k-nearest neighbour classifier to classify red lesions from the connected vasculature. Acharya *et al.* [4] used morphological techniques to detect the blood vessels and exudates. An edge detection technique followed by a mathematical morphology was used to detect microaneurysms. Walter *et al.* [5] proposed an automatic method for the detection of microaneurysms based on diameter closing for detecting candidates followed by feature extraction to automatically classify candidates into real microaneurysms and other objects. A decision support system for early detection of microaneurysms was proposed by Kahai *et al.* [6]. This detection method is based on a binary-hypothesis testing problem by using the Bayes optimality criteria. A bilinear top-hat transformation and matched filter are employed by Spencer *et al.* [7] to provide an initial segmentation of candidate microaneurysms from the image. Then a region-growing algorithm is used to delineate each marker object and subsequent analysis of candidate features for final detection of microaneurisms.

In this paper, an automated method for the detection of red lesions is proposed using a morphological technique to segment red lesion candidates and a rule-based classifier to discriminate actual red lesions from spurious red lesions. The method is divided into three stages. The first stage consists of shade correction and normalization of the green channel image. In the second stage, a method for detection of retinal blood vessels is proposed to serve in refining red lesion candidates. The third stage comprises the red lesion detection which is based on candidate segmentation, blood vessel removal, feature extraction and classification.

II. Methodology

A. Pre-processing

This stage aims to prepare the image with better properties by reducing differences in illumination and increasing the

visual contrast between retinal features and the background. The colour fundus image is initially resized to one of the standard sizes, 640×480 pixels, if it is already in these proportions; otherwise the width is resized to 640 pixels while the aspect ratio is preserved. This allows the proposed method to be applied to a variety of databases irrespective of resolution. As lesions and other retinal features appear more contrasted in the green channel component than those in the other channels of the colour image [8], we used the green channel image in all subsequent steps. To remove illumination variations in the image, a shade correction operation was used. This was carried out by smoothing the green channel image with a median filter of a large scale neighborhood window and subtracting the filtered image from the original image. This operation has the effect of leaving features whose scale is smaller than the filter scale such as red lesions and blood vessels. The resulting image is normalized to achieve a shade corrected image with the same maximum and minimum levels as the original image.
Fig. 2(a) and 2(b) illustrate a green channel image before and after the pre-processing operation respectively.

B. Red lesion detection

Since the lesions are leaks from the side of swelling tiny blood vessels [2], they tend to have spherical shape with diameters greater than the feeding blood vessels. Hence, they have particular pattern shapes extremely different from other retinal features, like blood vessels. In this section, objects that are most likely red lesions are extracted, as candidates, using a morphological technique followed by refining from vessels and then classification to remove other likely artifact types.

1) Candidate segmentation

The key idea of extraction of candidate regions is that red lesions have a particular profile that differs from other red regions like the blood vessels. Firstly, red lesions are segmented from the background by using a flood-fill operation on the background pixels of the pre-processed image, followed by subtracting the pre-processed image from the result of filling operation. These morphological operations can give high degree of discrimination between linear and circular shapes and then they are suitable for discriminating red lesions from blood vessels. Secondly, the resulting image was converted to a binary form with a threshold α_1. This threshold is calculated dynamically based on the mean intensity of the pre-processed image (m_{prd}). Experimental results showed that the threshold value $0.12 \times m_{prd}$ is most suitable for achieving a trade-off between true positives and false positives (FPs). Moreover, we took into account that most red lesions should be detected with this α_1 as any red lesion object missing, in this stage, could not be reinstated that may affect the method performance. Fig. 2(c) and 2(d) show results of candidate segmentation before and after the thresholding respectively.

Although morphological operations, used for candidate extraction, can give high degree of discrimination between linear and circular shapes, the resulting image may still include some vessels and other artifacts. The fovea appears with similar features as red lesions and hence it is mostly detected as a red lesion. Moreover, some contrasted features inside the optic disk occasionally appear as red lesions. To refine the resulting image from such artifacts, the blood vessel image, optic disk mask image and fovea mask image were subtracted from the resulting candidate image to obtain a new image with red lesions and few spurious objects which could be removed by a classification operation. The localization of the optic disk and fovea were obtained by using the methods described by Niemeijer *et al*. [9] and Li *et al.* [10] respectively, while a method of blood vessel detection is proposed in Section B-3. Fig. 2(e) illustrates the binary candidate image after the refining process.

2) Feature extraction

The result of candidate segmentation may include spurious red lesions. Consequently, a set of 9 features was calculated for each candidate. In the following features G and P refer to the green channel image and the pre-processed image respectively.

1) The aspect ratio $r = l \,/\, w$, where l is the length of the longest axis of the candidate and w is the width of the candidate on the axis perpendicular to the longest axis.
2) The area $a = \sum_{j \in X} 1$, X is a set of pixels in the candidate.
3) The perimeter p which is approximated using the chain-code of the candidate. $p = n_o\sqrt{2} + n_o$, where n_o is the number of each odd and even chain-codes.
4) The circularity $c = 4\pi a / p^2$. It gives a measure of roundness and smoothness of the candidate.
5) The eccentricity e which is a ratio of the distance between the foci of the ellipse and its major axis length. This value is between 0 (for a circle) and 1 (for a line segment).
6) The mean intensity of the candidate in G, $m_{grn} = i_{grn}/a$.
7) The inner standard deviation of G, σ_{grn}.
8) The mean intensity of the candidate in P, $m_{prd} = i_{prd}/a$.
9) The inner standard deviation of P, σ_{prd}.

where i_{grn} and i_{prd} refer to the total intensity of the green channel component image and the pre-processed image respectively.

3) Blood vessel detection

The main difficulty for red lesion detection is the resemblance and interference in colour intensity between them and the blood vessels which are spread throughout the retina. Therefore, blood vessel image can be detected and used to refine resulted red lesion image. Retinal blood vessels are dark linear structures with different ranges of diameter, length and orientation. Consequently, multi-scale techniques are suitable to isolate features of blood vessels from the background. For this, we propose a computationally fast method by applying morphological closing operation to the pre-processed image twice with two different scales of disk-shaped structuring elements. The radius of the larger disk at the adopted resolution is 8 pixels and the smaller is 2 pixels. Then the closed image with the smaller structuring element is subtracted from the larger one followed by thresholding to obtain an initial binary blood vessel image. It is found empirically that the suitable threshold (α_2) is about 90% of the maximum intensity.

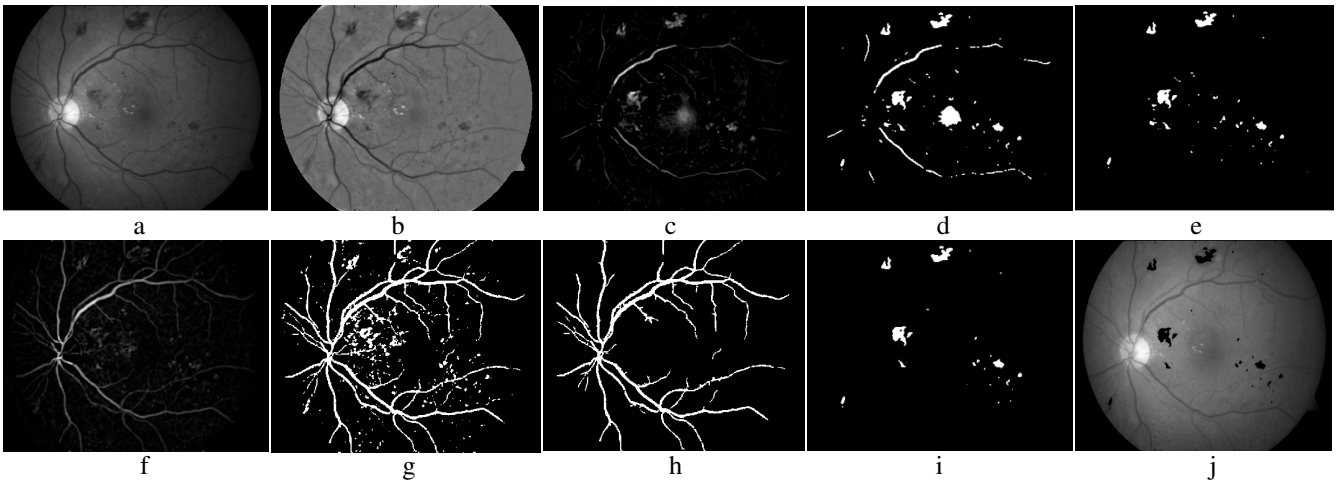

Fig. 2 Results of methodology steps. (a) Green channel image. (b) Image after pre-processing. (c) Result of morphological operation on the pre-processed image. (d) Binarisation of the morphological operation result. (e) Image after refining by removing the vascular, optic disc and fovea. (f) Result of multi-scale thresholding technique. (g) Binarisation of multi-scale technique result. (h) Final blood vessel image after classification. (i) Image after classification (final binary image of red lesion detection). (j) The binary result superimposed on the original gray image.

The rationale behind this approach is that the closing operator performs dilation followed by erosion operations. The dilation process expands bright regions and shrinks small dark regions, and the subsequent erosion operator will shrink the dilated bright regions to their original sizes while the shrunk dark regions do not respond to this erosion operation. Thus, a subtraction process between the two resulting images will highlight the dark regions, including the blood vessels. Fig. 2(f) and 2(g) illustrate the results of the multi-scale technique before and after the thresholding.

Due to the variability of the condition and quality of the images, the initial blood vessel image may include other types of dark regions. Discrimination of the blood vessels from these other regions can be achieved using a rule-based classifier. Our proposed method for the classification is based on features of region properties, such as aspect ratio, area, circularity and eccentricity. The final binary image of the blood vessels is obtained by selecting objects which comply with properties of blood vessels. Experimentation with many images based on information of hand-labeled results has shown that the following relations: $r \geq 3$, $a > 50$, $c < 0.5$ and $e > 0.8$ are most suitable to classify true blood vessels and discard other artifacts. Fig. 2(h) illustrates the final blood vessel image.

4) Classification

The aim of candidate classification is to classify each candidate as either an actual red lesion or spurious red lesion. A series of experiments on feature selection and red lesion classification were performed using a rule-based classifier. This system is based on a number of quantities and logical rules. These rules, in our work, are empirically derived from the data of training by a series of comparison between many pairs of features from the feature vector and looking for functions of every two features. A number of rules were incorporated directly into image analysis and quantification program. Then they are established by a number of constraint criteria, leading to an efficient classifier. An example of a rule-based analysis is illustrated in the classification rules used in Section B-3, where constraint criteria are based on the shape and size relations. For the classification of red lesion candidates, the features described in Section B-2 were used to set a number of rules which comply with properties of red lesions as constraint criteria. Fig. 2(i) illustrates the final binary red lesion image after the classification, while Fig. 2(j) shows the final binary result superimposed on the gray image.

III. Results and Discussions

We used a set of 249 retinal images from different sources to train and test the proposed method. The sources of the images are as follows: a set of 30 retinal images (set 1), used as training set, is from the Massidor database [8], of which 21 images contain red lesions. These manually annotated images were captured at 45^{o} field of view and a resolution of 640×480 pixels. Testing was carried out using a different set of 219 images from different databases. This test set consists of 89 images taken from the DIARETDB1 database [11], of which 46 contained red lesions, and 130 images taken from the DIARETDB0 database [12], of which 110 contained red lesions. These images were captured at 50^{o} field of view and a size of 1500×1152 pixels.

Images of the test set were annotated by ophthalmologists that can be used for testing the proposed method at two levels of evaluation: the lesion level and the image level. Performance of the proposed method was assessed quantitatively by applying logical comparison to the binary results of the proposed method and the annotated images (gold standard). The performance of our method is evaluated, in both lesion and image levels, by comparing the sensitivity and specificity with other related works as shown in Table 1. The proposed method has a distinctive sensitivity of lesion level compared to the other works. Anyhow, the other measures are still favourable in comparison to the other related works and can be improved by decreasing FPs. Although, we have been comparing the performance of the proposed method with those works of robust techniques, but

TABLE 1
PERFORMANCE MEASURES OF VARIOUS RELATED WORKS

	At lesion level		At image level	
Reference	SE%	SP%	SE%	SP%
Niemeijer *et al.* [3]	87	--	100	87
Acharya *et al.* [4]	82	86	--	85.9
Walter *et al.* [5]	88.5	98.9	--	--
Kahai *et al.* [6]	--	--	100	63
Spencer *et al.* [7]	83.6	99.2	--	--
Proposed method	89.7	98.6	98.8	86.2

SE = Sensitivity, SP = Specificity.

this may not be fair because these previous related works had tested their methods with different sources of databases than ours. Due to the lack of publicly available databases which can be used by many researchers, it is difficult to find many techniques tested by a same database.

To investigate the importance of refining by blood vessel removal, many experiments have been carried out with and without vessel removal. It is found that the method with vessel removal can achieve results with clearly lower undesirable FPs but with slight effect on sensitivity. Thus, blood vessel removal is feasible because it can remove many spurious red lesions with minor effect on sensitivity.

The algorithm performance at lesion level was assessed with different threshold α_1 using the following set:
$\alpha_1 \in (0.06,0.08,0.10,0.12,0.14,0.16,0.18,0.20,0.22)m_{prd}$
The test results indicate that $0.12 \times m_{prd}$ achieves the best compromise between FPs and sensitivity as shown in Fig. 3.

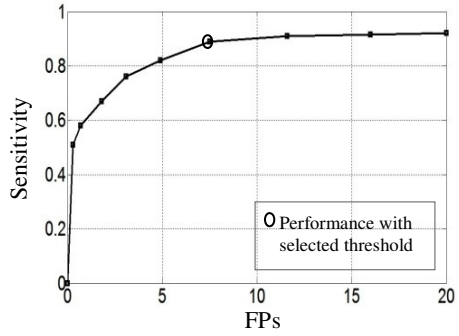

Fig. 3 Effect of the threshold $\alpha_1$on balance between FPs and sensitivity.

For more clarification to the performance of the proposed method, three examples of results are shown in Fig. 4.

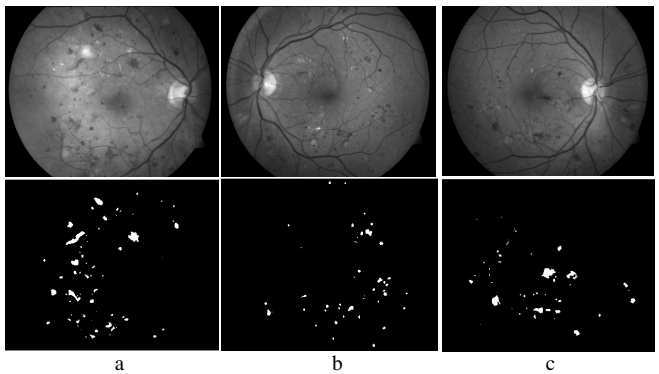

a b c

Fig. 4 Examples of images and their binary red lesion detection images by the proposed method. (a) Example 1. (b) Example 2. (c) Example 3.

IV. CONCLUSIONS

In this work, a novel framework for detection of red lesions has been proposed. The proposed method is based on candidate segmentation by applying morphological operations and red lesion classification using a rule-based classifier. The majority of FPs detected during candidate segmentation is due to the blood vessels. Hence, domain knowledge of the blood vessels is important to refine the result before the classification step. For this a new method for blood vessel detection has also been proposed to refine the candidate segmentation result. Experimental results show that masking the blood vessels from the image before the classification step can decrease the number of FPs and reduce the complexity of the classifier. A limitation in our work arises due to missing red lesions inside fovea during refining process. Future work will address improvements to this system by developing the feature extraction and classification and by detecting red lesions inside the fovea.

ACKNOWLEDGMENT

The authors would like to thank the DIARETDB1 Database Centre [11], the DIARETDB0 Database Centre [12] and the Centre of Mathematical Morphology, Mines Paris Tech. [8] for their co-operation in providing retinal images. Hussain F. Jaafar would like to acknowledge the financial support of the Iraqi government for this research.

REFERENCES

[1] D. S. Fong, L. Aiello, T. W. Gardner, G. L. King, G. Blankenship, J. D. Cavallerano, F. L. Ferris, and R. Klein, "Diabetic retinopathy," *Diabetes Care*, vol. 26, no.1, pp. 226-229, 2003.

[2] Facts about diabetic retinopathy, National Eye Institute, available from: http://www.nei.nih.gov/health/diabetic/retinopathy.asp

[3] M. Niemeijer, B. V. Ginneken, J. Staal, M. S. Suttorp-Schulton and M. D. Abramoff, "Automatic detection of red lesions in digital color fundus photograph," *IEEE Trans Med Imaging*, vol. 24(5), May 2005.

[4] U. R. Acharya, C. M. Lim, E. Y. K. Ng, C. Chee, and T. Tamura, "Computer-based detection of diabetes retinopathy stages using digital fundus images," *J. Engineering in Medicine*, 223 , pp. 545-553, 2009.

[5] T. Walter, P. Massin, A. Erginary, R. Ordonez, C. Jeulin, and J. Klein, "Automatic detection of microaneurysms in color fundus images," *Medical Image Analysis*, vol. 11, pp. 555-566, 2007.

[6] P. Kahai, K. R. Namuduri, and H. A. Thompson, "A decision support framework for automated screening of diabetic retinopathy," *Int. J. Biomed. Imaging*, pp. 1-8, 2006.

[7] J. Spencer, J. A. Oslon, K. C. McHardy, P. F. Sharp, and J. V. Forrester, "An image-strategy for the segmentation and quantification of microaneurysms in fluorecein angiograms of the ocular fundus," *Comput. Biomed. Res*., vol. 29, pp. 284-302, 1996.

[8] T. Walter, J. C. Klein, P. Massin, "A contribution of image processing to the diagnosis of diabetic retinopathy detection of exudates in colour fundus images of the human retina," *IEEE Trans Med Imaging,* vol. 21, pp. 1236-43, 2002.

[9] M. Niemeijer, M. D. Abramoff, and B. V. Ginneken, "Fast detection of the optic disk and fovea in color fundus photographs," *Med Image Anal*, vol. 13, pp. 859-870, 2009.

[10] H. Li, O. Chutatape, "Automated feature extraction in color retinal images by a model based approach," *IEEE Trans Biomed Eng,* vol. 51(2), pp. 246-254, 2004.

[11] T. Kauppi, V. Kalesnykiene, J. K. Kamarainen, L. Lensu, I. Sorri, A. Raninen, R. Voutilainen , H. Uusitalo, H. Kalviainen, J. Pietila, "DIARETDB1: diabetic retinopathy database and evaluation protocol," *Technical report,* Faculty of Medicine, University of Kuopio, Finland, 2007.

[12] T. Kauppi, *et al.*, "DIARETDB0: Evaluation database and morphology for diabetic retinopathy algorithm," *Technical report*, Lappeenranta University of Technology, Finland, 2006.